

Quasi-Phase-Matched Difference Frequency Generation Devices with Annealed/Proton-Exchanged LiNbO₃ Waveguides Buried by Reverse Proton Exchange

Masatoshi FUJIMURA, Toru MURAYAMA and Toshiaki SUHARA

Department of Electronic Engineering, Graduate School of Engineering, Osaka University, 2-1 Yamada-oka, Suita, Osaka 565-0871, Japan

(Received August 2, 2004; revised September 8, 2004; accepted September 29, 2004; published November 12, 2004)

Annealed/proton-exchanged LiNbO₃ waveguides buried by reverse proton exchange were studied and applied to quasi-phase-matched difference frequency generation (DFG) devices to improve their efficiency. A device of 3.1 cm length was fabricated and characterized. In preliminary second harmonic generation experiments, four-fold improvement in the normalized efficiency was demonstrated. In DFG wavelength conversion experiments, conversion efficiency of -9 dB for pump power of 12 mW was achieved. The corresponding normalized DFG efficiency was 1000%/W, which is, to the best of the authors' knowledge, the highest value ever reported. [DOI: 10.1143/JJAP.43.L1543]

KEYWORDS: lithium niobate, quasi-phase matching, difference frequency generation, wavelength conversion, buried waveguides, nonlinear optics, proton exchange

LiNbO₃ waveguide quasi-phase-matched (QPM) difference frequency generation (DFG) devices have been studied actively for application to wavelength converters for dense wavelength division multiplexing optical communication networks because of properties such as wide wavelength bandwidth, ability of simultaneous conversion of multiple wavelength signals, and high transparency to signal format.^{1,2)} Improvement of conversion efficiency is an important requirement for practical application.

The efficiency can be improved by increasing the overlap of guided mode profiles of interacting waves. An annealed/proton-exchanged (APE) LiNbO₃ waveguide with a high-index cladding layer was used to increase the overlap, and efficiency improvement was achieved.³⁾ Another approach is to utilize waveguides buried in the crystal. APE:LiNbO₃ waveguides buried by reverse proton exchange (RPE) were proposed and demonstrated.^{4,5)} A second harmonic generation (SHG) device with a RPE-buried waveguide of 3.3 cm length exhibited a high normalized SHG efficiency of 1600%/W for pumping at a wavelength of 1.54 μm.⁶⁾

In this work, we studied the fabrication of RPE-buried APE waveguides for QPM-DFG devices and demonstrated DFG wavelength conversion with an efficiency of -9 dB for 12 mW pump power in a prototype device of 3.1 cm length.

The RPE-buried APE:LiNbO₃ waveguide QPM-DFG device is shown in Fig. 1. A signal wave (wavelength: $\lambda_s \sim 1.5 \mu\text{m}$, frequency: ω_s , power: P_s) and a pump wave ($\lambda_p \sim 0.8 \mu\text{m}$, ω_p , P_p) are coupled in a buried waveguide with a domain inverted grating for QPM. The QPM-DFG wave ($\lambda_D \sim 1.5 \mu\text{m} \neq \lambda_s$, $\omega_D = \omega_p - \omega_s$, P_D) is generated to enable wavelength conversion from λ_s to λ_D . When P_D is small, the normalized DFG efficiency, $\eta_{DF} \equiv P_D/(P_s P_p)$,

under QPM is approximately given by²⁾

$$\eta_{DF} = \kappa^2 L^2, \quad (1)$$

$$\kappa = \frac{\omega_D \epsilon_0}{\pi} \iint E_D^* d_{33} E_p E_s^* dx dy, \quad (2)$$

where κ is the nonlinear coupling coefficient, d_{33} the nonlinear-optic coefficient. E_D , E_p , and E_s represent guided mode profiles for the DF, pump, and signal waves, respectively. κ increases in proportion to the overlap of the guided mode profiles in the cross section of the waveguide, and η_{DF} increases in proportion to κ^2 .

Conventional non-buried APE waveguides have index maxima at the crystal surface, and the index profiles of the waveguides are highly asymmetric in the depth direction. Therefore, the peaks of the mode profiles for different wavelengths are considerably far from one another. Hence, the overlap cannot be large. On the other hand, buried APE waveguides have index maxima below the crystal surface, and the index profiles are fairly symmetric. Therefore, the mode profiles in buried waveguides are close to symmetric, and the peaks are closer. Then mode overlap can be greater, and higher conversion efficiency is expected.

Immersion of APE:LiNbO₃ in Li⁺-rich melt (eutectic salt of LiNO₃:KNO₃:NaNO₃ with mol ratio of 37.5:44.5:18.0⁵⁾) causes replacement of H⁺ in APE:LiNbO₃ with Li⁺ in the melt. This reverse proton exchange (RPE) process reduces the H⁺ concentration in the vicinity of the surface, and the H⁺ concentration maximum is pushed below the crystal surface. Thus the waveguide is buried.

Al masks with channel openings of 5 μm width were formed on Z-cut LiNbO₃ crystals, and they were immersed into benzoic acid at 200°C for 1.5 h for proton exchange and annealed in oxygen atmosphere at 370°C. These conditions were the same as the typical conditions for non-buried APE waveguide fabrication. After the APE treatment, RPE was carried out in the eutectic salt at 326°C in the setup shown in Fig. 2. It was found, in preliminary experiments, that stirring of the salt is essential to obtain uniform waveguides. RPE-buried APE channel waveguides were fabricated for various annealing and RPE durations. The other conditions including the initial PE conditions were not varied, and therefore, totally optimized conditions were not obtained in this work. Near-field patterns of the guided modes were measured at

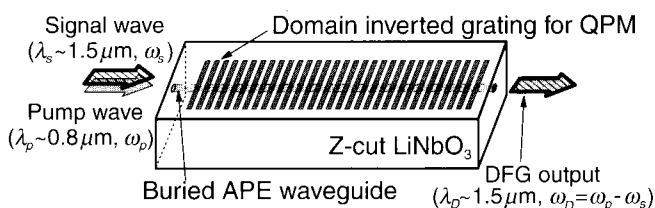


Fig. 1. RPE-buried APE:LiNbO₃ waveguide QPM-DFG device.

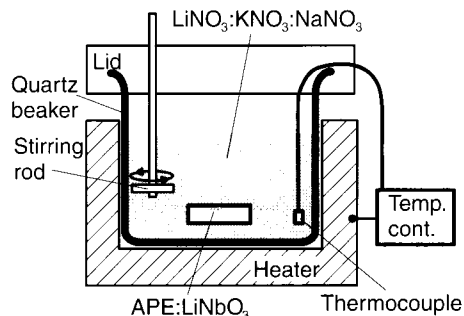
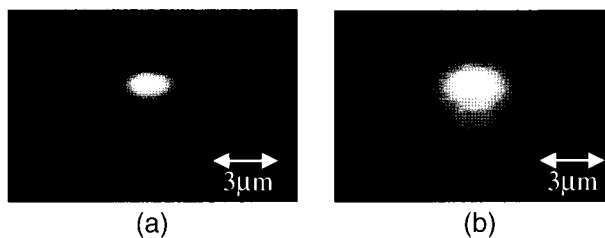


Fig. 2. Setup for reverse proton exchange.

Fig. 3. Near-field patterns of guided modes in (a) RPE-buried and (b) non-buried APE waveguides at 1.55 μm .

wavelengths of $\sim 1.55 \mu\text{m}$ and $\sim 0.8 \mu\text{m}$. Figures 3(a) and 3(b) show the pattern for the 1.55 μm wavelength in a buried waveguide fabricated with 1 h of annealing and 1 h of RPE and that in a non-buried waveguide fabricated by PE at 200°C for 1.5 h using a mask with channel openings of 5 μm width followed by annealing at 370°C for 4 h, respectively. The symmetry of the pattern was improved by RPE burial. The mode profiles in the depth direction for 1.6 μm and 0.8 μm wavelengths are shown in Fig. 4. The RPE-buried waveguide provided greater mode overlap. The distances between the peaks of the profiles were 0.41 μm and 1.23 μm for the RPE-buried and the non-buried waveguides, respectively. The nonlinear coupling coefficients calculated using the measured mode profiles and $d_{33} = 32 \text{ pm/V}$ were $\kappa = 1.33 \text{ W}^{-1/2} \text{ cm}^{-1}$ and $\kappa = 0.77 \text{ W}^{-1/2} \text{ cm}^{-1}$ for buried and non-buried waveguides, respectively. Therefore, the ratio of the improvement in the normalized efficiency is estimated to be as large as approximately 3 ($= (1.33/0.77)^2$).

A QPM-DFG device with the RPE-buried APE waveguide

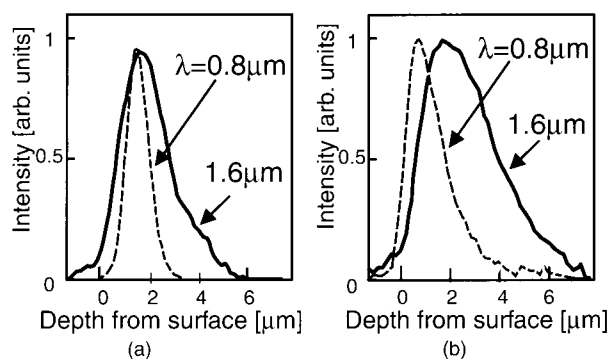
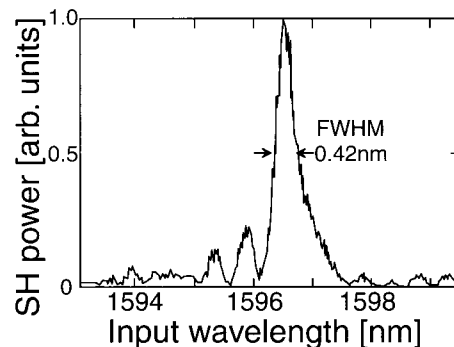
Fig. 4. Mode profiles in depth direction for $\lambda = 0.8 \mu\text{m}$ and 1.6 μm in (a) RPE-buried and (b) non-buried waveguides.

Fig. 5. SH power dependent on input wavelength.

was fabricated. A domain inverted grating with period of 15.5 μm and length of 3.1 cm was fabricated in Z-cut LiNbO₃ crystal 0.5 mm thick by applying a voltage pulse of 11.4 kV amplitude through a periodic electrode.⁷⁾ A RPE-buried APE waveguide was fabricated as described in the previous section.

Simple SHG experiments were carried out for preliminary device characterization because the normalized DFG efficiency η_{DF} for nearly degenerate DFG ($\lambda_s \sim \lambda_D$) is theoretically equal to the normalized SHG efficiency η_{SH} . An input wave from an external-cavity wavelength-tunable laser diode was coupled in the device and the output SH power was measured. The SH power dependent on the input wavelength is shown in Fig. 5. QPM-SHG was achieved at an input wavelength of 1596.5 nm. The measured FWHM wavelength bandwidth of 0.42 nm is close to the theoretical prediction of 0.44 nm. This agreement suggests good uniformity of the waveguide and the QPM grating. Figure 6 shows the SHG efficiency dependent on the input wave power. The normalized SHG efficiency, i.e., slope of the line in the figure, was $\eta_{\text{SH}} = 1400\%/W$. The corresponding coupling coefficient is $\kappa = 1.2 \text{ W}^{-1/2} \text{ cm}^{-1}$. This is close to the value estimated using the mode profiles. The values for a reference device with a non-buried APE waveguide were 320%/W and $0.60 \text{ W}^{-1/2} \text{ cm}^{-1}$.⁸⁾ The device with a RPE-buried waveguide achieved a normalized efficiency four times as high as that of the reference device with the non-buried APE waveguide. The ratio of the efficiency improve-

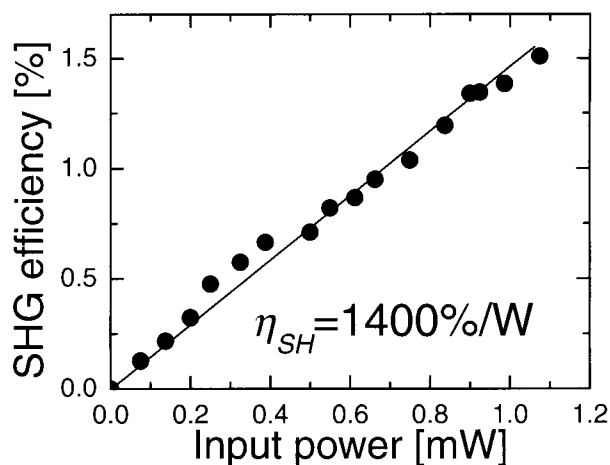


Fig. 6. SHG efficiency dependent on input power.

ment obtained in the experiments was larger than that of the above estimation using the measured mode profiles. This seems to be due to the improved uniformity in the waveguide and/or the domain-inverted grating of the recently-fabricated device over that of the previously-fabricated device.

The actual DFG normalized efficiency η_{DF} is usually smaller than the SHG normalized efficiency η_{SH} because of the factors neglected in the theoretical model, *e.g.*, photo-refractive effect and pump power propagation in the higher guided modes. DFG wavelength conversion experiments were carried out. A pump wave from a Ti:Al₂O₃ laser ($\lambda_p = 0.80\ \mu\text{m}$) and a signal wave from a laser diode were combined using a dichroic beam splitter and coupled in the device. A spectrum of the output waves was measured using an optical spectrum analyzer. Wavelength conversion of $-9\ \text{dB}$ efficiency was obtained, as shown in Fig. 7, for a pump power of 12 mW. The conversion efficiency corresponds to a normalized efficiency of $\eta_{DF} = 1000\%/W$. This is the highest normalized DFG efficiency ever reported to the best of our knowledge, although it is smaller than the normalized SHG efficiency reported in ref. 6.

The fabrication of RPE-buried APE:LiNbO₃ waveguides was studied, and high performances of a QPM-DFG device with the buried waveguide were demonstrated. Further efficiency improvement can be achieved by increasing the interaction length.

This work was supported by Grant-in-Aid from the Ministry of Education, Culture, Sports, Science, and Technology (MEXT) and by Handai Frontier Research Center (FRC).

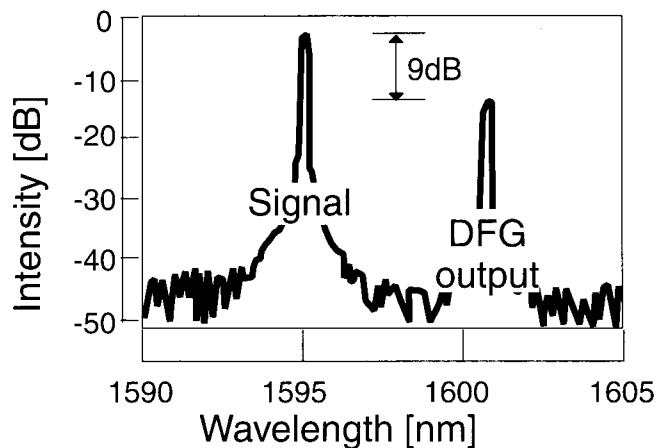


Fig. 7. Spectrum of output waves in DFG experiments.

- 1) C. Q. Xu, H. Okayama, K. Shinozaki, K. Watanabe and M. Kuwahara: *Appl. Phys. Lett.* **63** (1993) 1170.
- 2) T. Suhara and M. Fujimura: *Waveguide Nonlinear-Optic Devices* (Springer-Verlag, Berlin, 2003) Chaps. 3 & 9.
- 3) D. Sato, T. Morita, T. Suhara and M. Fujimura: *IEEE Photon. Technol. Lett.* **15** (2003) 569.
- 4) J. L. Jackel and J. J. Johnson: *Electron. Lett.* **27** (1991) 1360.
- 5) Y. Korkishko, V. A. Fedrov, T. M. Morozova, F. Caccavale, F. Gonella and F. Segato: *J. Opt. Soc. Am. A* **15** (1998) 1838.
- 6) K. R. Parameswaran, R. K. Route, J. R. Kurtz, R. V. Roussev, M. M. Fejer and M. Fujimura: *Opt. Lett.* **27** (2002) 179.
- 7) K. Kintaka, M. Fujimura, T. Suhara and H. Nishihara: *J. Lightwave Technol.* **14** (1996) 462.
- 8) D. Sato, T. Morita, K. Shio, M. Fujimura and T. Suhara: *Ext. Abstr. (49th Spring Meet. 2002); Jpn. Soc. Appl. Phys. Related Soc., 27pZS4.*